

## SILICA MEMBRANES – BASIC PRINCIPLES

André AYRAL, Anne JULBE, Stéphanie ROUALDES, Vincent ROUESSAC,  
Jean DURAND and Béatrice SALA<sup>‡</sup>

Institut Européen des Membranes, UMR No. 5635 CNRS-ENSCM-UMII  
CC047, Université Montpellier II, Place Eugène Bataillon,  
34095 Montpellier cedex 5, France  
e-mail: Andre.Ayral@iemm.univ-montp2.fr

Received: Sept. 14, 2005

### Abstract

Basic principles on amorphous silica membranes are presented. The advantages and disadvantages of microporous amorphous silica are discussed to explain its use as separative membranes for specific applications. The synthesis methods are reported and examples of silica membrane designs are given.

*Keywords:* membrane, silica, microporosity, gas separation.

### 1. Introduction

Silica (SiO<sub>2</sub>) exhibits unique properties related to the ability of its elemental bricks, i.e. SiO<sub>4</sub> tetrahedra, to be connected together to give rise to a large number of different amorphous or crystallized solids which can be microporous, mesoporous or macroporous (*Table 1*). In comparison with other common single oxides like alumina (Al<sub>2</sub>O<sub>3</sub>), titania (TiO<sub>2</sub>) or zirconia (ZrO<sub>2</sub>), silica can be more easily prepared as ultra or super-microporous thin layer and thus used for molecular sieving applications. Zeolites which are mainly silica or silica-based crystallized solids with structural ultra-microporosity will be presented elsewhere.

This paper will be focused on basic principles on microporous amorphous silica membranes. Microporous amorphous silica exhibits a weak stability in aqueous solutions or wet steams which limits its use as separative membranes to specific applications.

Several old and recent reviews on inorganic membranes are available with parts devoted to the synthesis and applications of microporous amorphous silica membranes [1]-[4]. The main current developments deal with *gas separation* applications, in particular hydrogen separation. The thermal stability of silica membranes compared to organic and hybrid layers and their interconnected porosity inside a stiff oxide skeleton enable to reach very good permeability-selectivity balances. For instance, H<sub>2</sub> permeance of the order of 10<sup>-6</sup> mol m<sup>-2</sup> s<sup>-1</sup> Pa<sup>-1</sup> with a H<sub>2</sub>/N<sub>2</sub> selectivity up to 100 has been recently reported in [4]. Other potential applications are *pervaporation* or *nanofiltration* of organic mixtures. In the case

---

<sup>‡</sup>Seconded to IEM from FRAMATOME

of nanofilters, it must be noted that requirements in terms of pore size are not so much restrictive and they enable to take advantage of the preparation of silica-based mixed oxide membranes to adapt the separative properties to the treated solvents [5].

After a brief introduction on the silica properties, this article will then present the synthesis methods used to prepare supported amorphous silica membranes. Finally, examples of silica membrane designs will be given.

*Table 1.* IUPAC classification of pores as a function of their size.

Micropores		Mesopores	Macropores
< 2 nm			
Ultra-micropores < 0.7 nm	Super-micropores > 0.7 nm	2 – 50 nm	> 50 nm

## 2. Amorphous Silica – Comparison with Other Oxides

Silica is a well-known glass former oxide whereas  $\text{Al}_2\text{O}_3$ ,  $\text{TiO}_2$  and  $\text{ZrO}_2$  are intermediate oxides in the classification of ZACHARIASEN [6]. They can not form by themselves glasses. The structure of silica glass consists of corner-sharing  $\text{SiO}_4$  tetrahedra covalently connected in a continuous infinite three-dimensional network having no long-range order.

Conventional preparation of glasses is performed by cooling melted solids, but amorphous phases can also be obtained at lower temperature from liquid solutions or gaseous mixtures. Amorphous phases are intrinsically metastable phases (*Table 2*). Thermal crystallization of intermediate oxides occurs at lower temperature compared to silica (*Table 2*). Crystallization is systematically associated with a microstructural change. In the case of microporous solids, it usually results in a significant enlargement of pore sizes. For high purity silica, crystallization can be delayed at very high temperature (close to the domain of thermodynamic stability of cristobalite). The thermal stability of porous silica is in fact limited by viscous flow sintering occurring at around  $800^\circ\text{C}$  in the case of microporous silica (*Fig. 1*).

## 3. Solubility of Amorphous Silica

The strong effect of temperature and pH on the solubility in water of amorphous silica (*Fig. 2*) clearly explains the limited use of silica membranes in aqueous solutions or wet atmospheres. In addition dissolution–redeposition phenomena are enhanced in the case of microporous materials associated with surface nanometric

Table 2. Structural data for common single oxides.

	SiO <sub>2</sub>	Al <sub>2</sub> O <sub>3</sub>	TiO <sub>2</sub>	ZrO <sub>2</sub>
Crystalline phase thermodynamically stable at room temperature	Quartz $\alpha$	Corundum	Rutile	Baddeleyite
Thermal crystallization of amorphous phases	in the range 900-1400 °C to cristobalite	in the range 400-700°C to transition aluminas	in the range 150-400°C to anatase or rutile	in the range 200-400°C to metastable cubic or tetragonal phases
Aging of amorphous phases in aqueous solution	no structural evolution	crystallization of hydroxides AlO(OH) or Al(OH) <sub>3</sub>	of crystallization of anatase or rutile	formation of hydrated oxyhydroxides

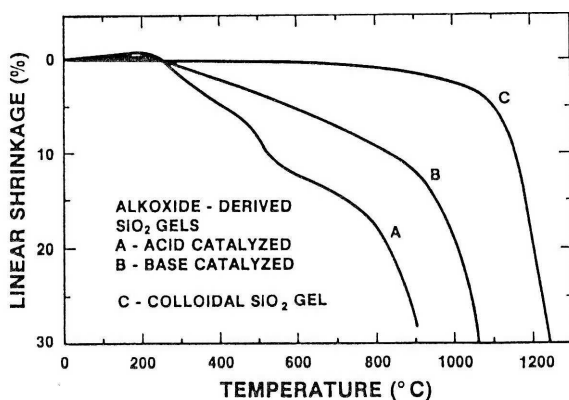


Fig. 1. Percent linear shrinkage for silica xerogels prepared by two-step acid-catalyzed hydrolysis of tetraethoxysilane, TEOS (water/TEOS molar ratio,  $r=5$ ) (A); two-step acid-base catalyzed ( $r=3.8$ ) (B); or destabilization of a particulate sol from Aerosil®(C). Heating treatments were performed at 2°C/min in air (from [7]).

radii of curvature (Fig. 3). The solubility strongly decreases for methanol-rich water-methanol mixtures whereas for pure alcohols, the solubility also decreases with the length of the alkyl chain (Table. 3). These last data contribute to explain the preservation of the silica microporosity in organic media.

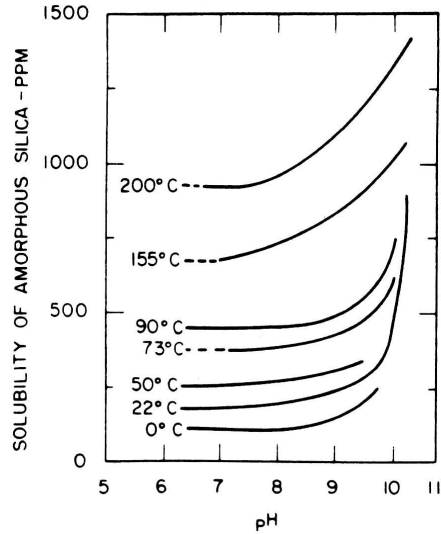


Fig. 2. Solubility of amorphous silica versus pH at different temperatures (from [8]).

Table 3. Solubility of amorphous silica in alcoholic solutions (from [8]).

Wt. % of methanol in water-methanol mixtures	Solubility at 25 °C mg L <sup>-1</sup>	Anhydrous alcohol	Solubility at 500 °C (ppm)
0	140	CH <sub>3</sub> OH	1890
25	75	C <sub>2</sub> H <sub>5</sub> OH	164
50	40	n-C <sub>3</sub> H <sub>7</sub> OH	8
75	15		
90	5		

## 4. Synthesis Methods

Homogeneous and defect-free amorphous silica films can be deposited on porous substrates using sol-gel routes or chemical vapor deposition (CVD) methods to produce asymmetric membranes. We will here discuss the synthesis conditions required to obtain microporous amorphous thin layers.

### 4.1. Sol-gel Routes

A convenient method to prepare microporous silica films starts from silicon alkoxides, Si(OR)<sub>4</sub>, as silica precursors [9]. The usual starting solutions are based on tetramethoxysilane, Si(OCH<sub>3</sub>)<sub>4</sub>, or tetraethoxysilane, Si(OC<sub>2</sub>H<sub>5</sub>)<sub>4</sub>, diluted in

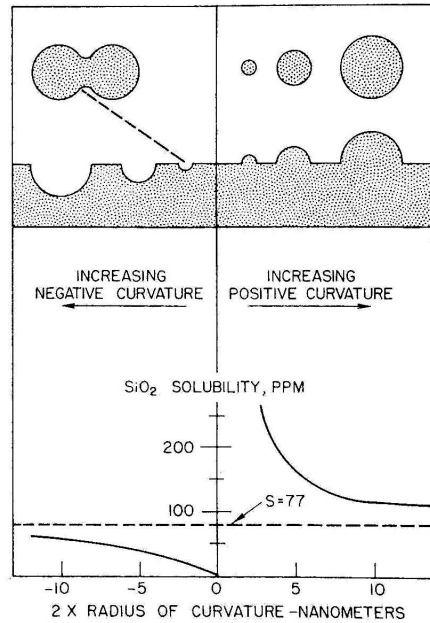
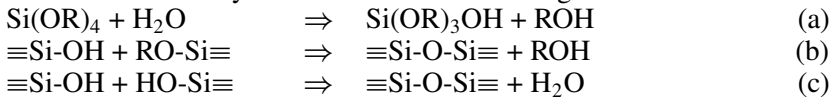
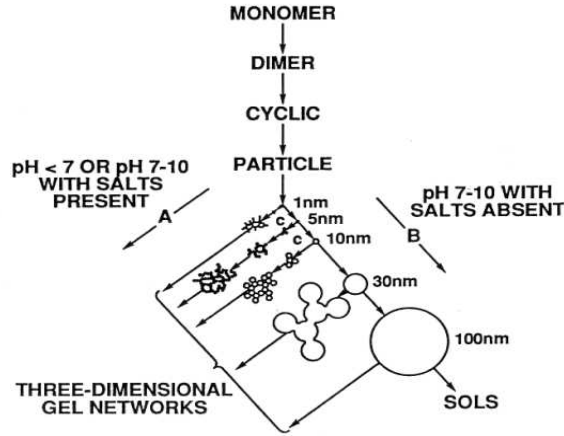


Fig. 3. Variation in solubility of silica with radius of curvature of surface. The positive radii of curvature are shown in cross-section as particles and projection from a silica surface. Negative radii are shown as depressions or holes in the silica surface, and in the crevice between two particles (from [8]).

methanol or ethanol, respectively. The formation of the oxide network results from the polymerization of the molecular precursor. The hydrolysis of the alkoxide (a) produces activated species and their condensation by alcoxolation (b) or oxolation (c) leads to a reticulation by formation of siloxane bridges  $\equiv\text{Si-O-Si}\equiv$ .



The hydrolysis and condensation reactions are catalyzed in acidic and basic media, respectively. As a function of the synthesis conditions, the polymerization process is modified identically as in aqueous medium (Fig. 4). The hydrolysis ratio (water/alkoxide molar ratio) is another important parameter. Acid catalysis induces long gelation times  $t_G$ . Coupled with a low hydrolysis ratio, it promotes the formation of linear polymers. The formation of dense clusters and short gelation times  $t_G$  are favoured by base catalysis. For a given alkoxide, differences in the synthesis conditions give rise to important differences for the porous texture of the final material as shown in Tables 4 and 5. Acidic conditions and short aging times before deposition must be preferred to get ultramicroporous layers.



*Fig. 4.* Polymerization behaviour of silica. In basic solution (B) particles in sol grow in size with decrease in numbers; in acid solution or in the presence of flocculating salts (A), particles aggregate into three-dimensional networks and form gels (from [8]).

*Table 4.* Influence of the hydrolysis method on the porous texture of polymeric silica gels derived from TEOS (from [7]).

Hydrolysis	Porosity (%)	Pore diameter (nm)	Specific surface area ( $\text{m}^2\text{g}^{-1}$ )
two-step acid-catalyzed	54	1-5	740
two-step acid-base-catalyzed	67	1-10	910
one-step base-catalyzed	70	1-20	515

*Table 5.* Aging of polymeric silica sols prior to film deposition ; effect on the porous texture of the resulting layers (from [10]).

Aging before deposition $t/t_G$	Porosity (%)	Average pore diameter (nm)	Specific surface area ( $\text{m}^2\text{g}^{-1}$ )
0 - 0.15	-	< 0.4	1 - 2
0.15	16	3.0	146
0.33	24	3.2	220
0.66	33	3.8	263
1	52	6.0	245

Templating strategies can also be advantageously applied to control the microporosity of the silica layers. A first way consists in templating molecules incorporated in the gelation medium, which are inert towards the chemical process leading to the inorganic network (route (c)-(d) in *Fig. 5*). An example illustrating such strategy deals with hydrolysis and condensation of silicon alkoxide in the presence of non-ionic surfactants and more precisely octyl aryl polyether alcohols with a general formula  $C_8H_{17}-C_6H_4-(OCH_2CH_2)_x-OH$  where  $x = 1, 3, 9-10$  or  $30$  [12]. The porous characteristics of the materials after a thermal treatment up to  $450^\circ C$  are reported in *Table 6*. While the materials synthesized without surfactant additives do not exhibit any measurable porosity by nitrogen adsorption, the results of *Table 6* clearly show that both the porous volume and the micropore size can be tailored by the added amount of surfactant and by the length of the polyoxyethylene chain.

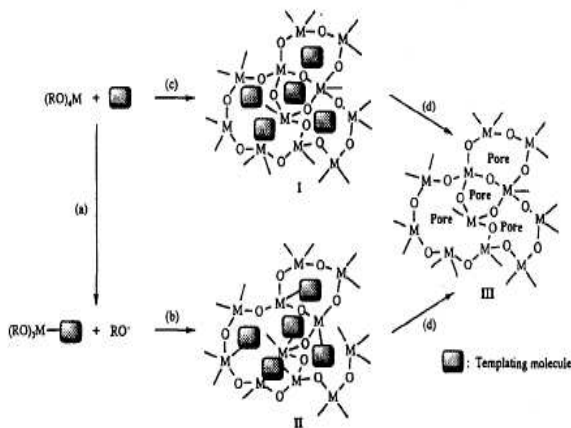


*Fig. 5.* Schematic illustration of the organic/inorganic template strategies (from [11]).

A second strategy consists in the use of modified alkoxides. A molecular group acting as template is covalently bounded to the Si atoms. This synthesis method is also schematically represented in *Fig. 5* (route (a)-(b)-(d)). The synthesis conditions are always selected in order to directly associate the porosity in the final material to the thermal elimination of the templating species during stage (d). Several papers were published on the improvement of microporous silica layers starting from mixtures of TEOS with a modified alkoxide like methyl-triethoxy-silane [13], methacryl-oxypopyl-trimethoxy-silane [14], phenyl-trimethoxy-silane or methyl-trimethoxy-silane [15].

Potential increase of the permeability in such microporous layers can be derived from hierarchical porous structures with non-interconnected extraporosity at a larger scale. In such conditions, the permselectivity of the membrane is still defined by the microporosity of the continuous phase. This strategy is illustrated with mesophase-templated silica membranes resulting in ordered but not interconnected

*Table 6.* Effect of addition of non-ionic surfactants ( $C_8H_{17}-C_6H_4-(OCH_2CH_2)_x-OH$ ) on the porous texture of unsupported silica layers measured from  $N_2$  adsorption – desorption isotherms (from [12]).

x	Surfactant/TEOS molar ratio	$S_{BET}$ ( $m^2g^{-1}$ )	Porous volume ( $cm^3g^{-1}$ )		Porosity (%)	Hydraulic pore radius (Å) range	mean
			total	microporous			
1	0.55	400	0.217	0.210	32.2	3-7	3.9
3	0.16	250	0.121	0.105	20.9	3-6	3.2
3	0.35	470	0.197	0.190	30.1	3-6	3.4
3	0.55	500	0.249	0.239	35.5	3-6	3.7
10	0.55	728	0.510	0.480	52.7	5-9	6.3
30	0.55	800	0.541	0.514	54.2	4-10	6.0

mesopores separated by microporous silica walls (*Fig. 6*) [16, 17].

Hydrophobic silica membranes can be prepared by one-pot methods from mixtures of TEOS and modified alkoxides avoiding further heat-treatment at temperatures higher than the thermal degradation of the organic groups directly bonded to Si (usually around  $250^\circ C$ ). Another route consists in surface grafting from liquids or gaseous phases, using experimental procedures derived from the preparation of chromatographic phases.

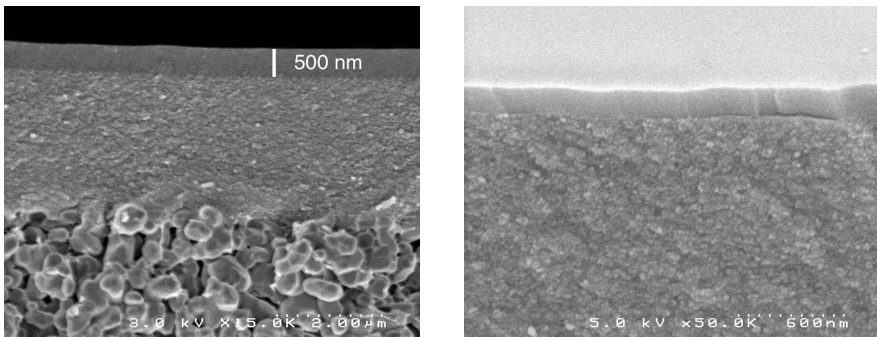


*Fig. 6.* Scanning electron microscope (SEM) images of 2D hexagonal (a) and 3D hexagonal mesoporous layers deposited on an asymmetric substrate with a  $\gamma$ -alumina top layer (from [16] and [17]).

#### 4.2. CVD Routes

Conventional CVD techniques (atmospheric pressure AP or low pressure LP) at high temperature ( $400-700^\circ C$ ) or Plasma Enhanced CVD methods (PECVD) at low



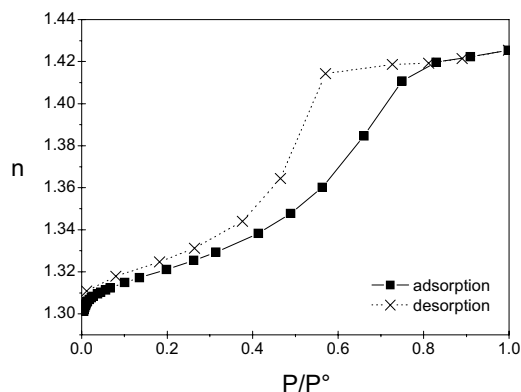


Fig. 7. Variation of the refractive index versus relative pressure of ethanol by ellipsometric porosimetry [20] for a  $\text{SiO}_x\text{C}_y\text{H}_z$  layer deposited by PECVD.

temperatures (Room Temperature–400°C) can also be easily used to prepare silica layers. The usual silica precursors are  $\text{SiH}_4$  or tetraethoxysilane (TEOS). They are mixed with  $\text{O}_2$ ,  $\text{N}_2\text{O}$  or  $\text{O}_3$  as oxidizing reactants. A large number of other organosilanes or alkoxy silanes can also be used. The conventional CVD coatings and the PECVD coatings performed with high energy conditions (i.e. for high values of the YASUDA and HIROTSU [18] composite parameter  $W/FM$  where  $W$  is the plasma power input,  $F$  the monomer flow rate and  $M$  the molecular weight of this monomer) give rise to rather dense silica layers with low carbon content [19].

Using PECVD and adapted silica precursors, film characteristics varying from amorphous silica to silicone-like polymers can be obtained by decreasing the  $W/FM$  ratio [19]. Moreover the use of porogen molecules enables to tune the porosity of these hybrid organic-inorganic layers (Fig. 7).

## 5. Silica Membrane Design

The objective of this last part is to briefly describe different configurations used to prepare silica membranes. Microporous silica layers are mainly deposited by dip-coating from sols on flat or tubular (mono or multichannel) asymmetric porous ceramic substrates [1]. The top layer of these substrates is usually a mesoporous  $\gamma$ -alumina layer. Improvement of both flux and selectivity can be reached by deposition of a first silica layer with  $\sim 1$  nm pore size and then a final 30 nm thick ultramicroporous silica top-layer (pore size 0.3-0.4 nm) (Fig. 8) [21]. The ceramic substrates can also be replaced by stainless steel porous tubes coated on one side with an intermediate ceramic layer prior to the silica film deposition [22]. A recent paper deals with microporous silica membranes deposited on the external

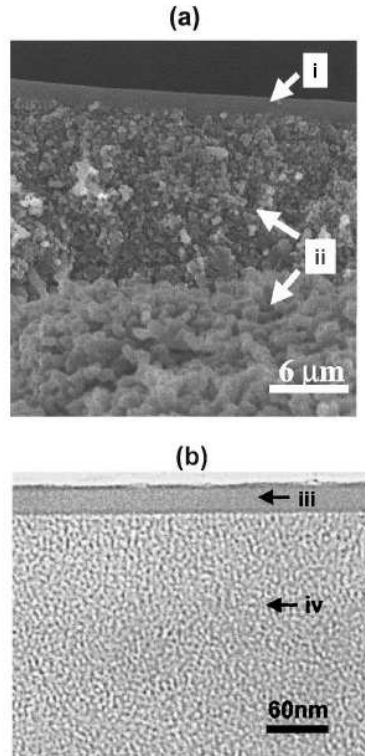


*Fig. 8.* Cross-sectional electron micrographs of an asymmetric membrane: (a) SEM overview — (i) SiO<sub>2</sub> membrane (see (b) in details) on top of  $\gamma$ -Al<sub>2</sub>O<sub>3</sub> layer, (ii) asymmetric  $\alpha$ -Al<sub>2</sub>O<sub>3</sub> support, and (b) TEM micrograph revealing the dual-layer silica membrane — (iii) ultramicroporous top layer, (iv) supermicroporous sublayer (from [21].)

side of ceramic hollow fibers (*Fig. 9*) [23]. Such configuration enables to reach a high membrane surface area/module volume ratio ( $>1000 \text{ m}^2 \text{ m}^{-3}$ ) compared to classical tubular membranes [23].

Conventional CVD or PECVD methods are also used to deposit silica layers on mesoporous  $\gamma$ -alumina top layers of ceramic substrates [24]–[26]. *Fig. 10* shows a reactor set-up developed to deposit PECVD films inside tubular supports. CVD silica layers can be deposited on porous Vycor glass supports (*Fig. 11*), [27, 28]. The resulting Nanosil membranes show rather low permeance ( $\sim 10^{-8} \text{ mol m}^{-2} \text{ s}^{-1} \text{ Pa}^{-1}$ ) for the small gas molecules (He, Ne and H<sub>2</sub>) at 873 K but high selectivity ( $\sim 10^4$ ) over larger gas molecules (CO<sub>2</sub>, CO, and CH<sub>4</sub>).

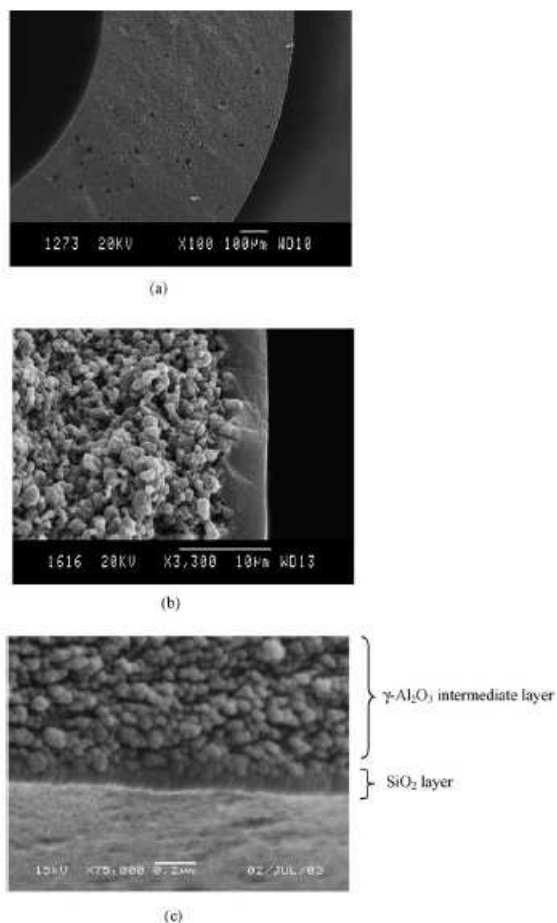
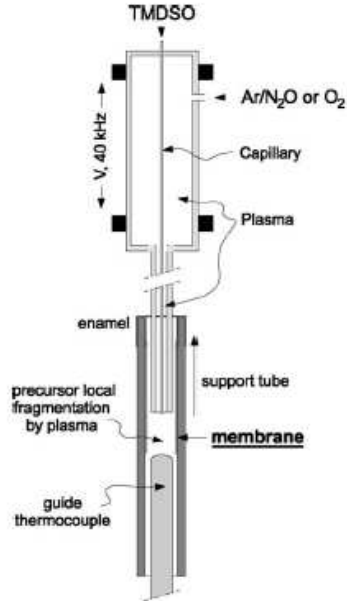


Fig. 9. SEM micrographs of the various layers constituting the ceramic hollow fiber: (a) cross-section substrate (magnification 100 x), (b) cross-section intermediate  $\gamma$ -Al<sub>2</sub>O<sub>3</sub> layers on top of substrate (magnification 3300 x), (c) cross-section silica membrane on the intermediate  $\gamma$ -Al<sub>2</sub>O<sub>3</sub> layers (magnification 75000 x) (from [23]).

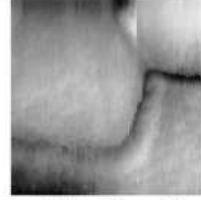
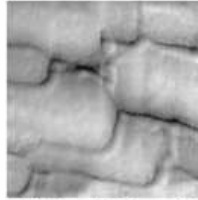
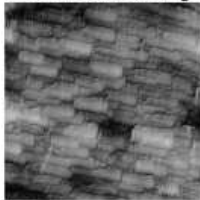
## 6. Conclusion

Taking into account the specific properties of silica and using convenient deposition methods with well-defined synthesis parameters, it is possible to prepare microporous silica membranes of particular interest for specific applications in high temperature gas separation, pervaporation or nanofiltration of organic media.



*Fig. 10.* Reactor set-up to deposit a membrane on the inner surface of a porous support tube by PECVD (from [26]).

### Untreated Vycor



### Nanosil

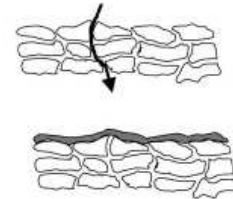
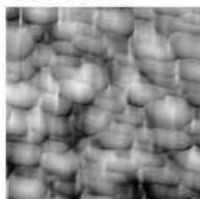


*Fig. 11.* Atomic force micrographs of the Vycor and Nanosil membranes (from [27]).

## References

- [1] *Fundamentals of Inorganic Membrane Science and Technology*, edited by A. J. Burgraff and L. Cot, Membrane Science and Technology Series, 4 (Elsevier, Amsterdam, 1996).
- [2] COT, L. – AYRAL, A. – DURAND, J. – GUIZARD, C. – HOVNANIAN, N. – JULBE A. – LARBOT, A. *Solid State Sciences* **3**[2] (2000) p. 313.
- [3] MEINEMA, H. A. – DIRRIX, R. W. J. – BRINKMAN, H. W. – TERPSTRA, R. A. – JEKERLE, J. – KÖSTERS, P. H., *Interceram* **54** (2005) p. 86.
- [4] SOMMER S. – MELIN, T., *Chemical Engineering and Processing* **44** (2005) p. 1138.
- [5] GUIZARD, C. – AYRAL, A. – JULBE, A. *Desalination* **147** (2002) p. 275.
- [6] ZACHARIASEN, W. H. *J. Am. Chem. Soc.* **54** (1932) p. 3841.
- [7] BRINKER, C. J. – SCHERER, G. W. *Sol-Gel Science, the Physics and Chemistry of Sol-Gel Processing* (Academic Press, Boston, 1990).
- [8] ILER, R. K. *The Chemistry of Silica*, Wiley (Interscience, New York, 1979).
- [9] AYRAL, A. – JULBE, A. – GUIZARD, C. – COT, L. *J. of the Korean Chem. Soc.*, **41** (1997) p. 566.
- [10] BRINKER, C. J. – FRYE, G. C. – HURD, A. J. – ASHLEY, C. S., *Thin Solid Films* **201** (1991) p. 97.
- [11] ROGER, C. – HAMPDEN-SMITH, M. J. *J. Mater. Chem.*, **2** (1992) p. 1111.
- [12] AYRAL, A. – BALZER, C. – DABADIE, T. – GUIZARD C. – JULBE, A., *Catalysis Today* **25** (1995) p. 219.
- [13] RAMAN, N. K. – BRINKER, C. J., *J. of Membrane Science* **105** (1995) p. 273.
- [14] KIM, Y. S. – KUSAKABE, K. – MOROKA S. – YANG, S. M., *Korean J. Chem. Eng.* **18** (2001) p. 106.
- [15] WEST, G. D. – DIAMOND, G. G. – HOLLAND, D. – SMITH - M. E. – LEWIS, M. H., *J. of Membrane Science* **203** (2002) p. 53.
- [16] KLOTZ, M. – AYRAL, A. – C. GUIZARD, G. – COT, L. *Sep. & Pur. Technol.* **25** (2001) p. 71.
- [17] KLOTZ, M. – BESSON, S. – RICOLLEAU, C. – BOSCH, F. – AYRAL, A., *Mat. Res. Soc. Symp. Proc.* **752** (2003) p. 123.
- [18] YASUDA, H. – HIROTSU, T., *J. Polym. Chem.* **16** (1973) p. 313.
- [19] ROUALDES, S. – VAN DER LEE, A. – BERJOAN, R. – SANCHEZ, J. – DURAND, J., *AICHE Journal*, **45** (1999) p. 1566.
- [20] REVOL, P. – PERRET, D. – BERTIN, F. – FUSALBA, F. – ROUESSAC, V. – CHABLI, A. – PASSEMARD, G. – AYRAL, A. *Journal of Porous Materials* **12** (2005) p. 113.
- [21] TSAI, C. Y. – TAM, S. Y. – LU, Y. – BRINKER, C. J. *J. of Membrane Science* **169** (2000) p. 255.
- [22] MANSUR, L. K. – BISCHOFF, B. L. – ADCOCK, K. D. – POWELL, L. E. – JUDKINS, R. R., *Proceedings ICIM<sub>8</sub>* – F. T. Akin and Y. S. Lin Eds, Adams Press Publisher, 8<sup>th</sup> Int. Conf. on Inorganic Membranes Cincinnati, Ohio, USA, July 18-21, 2004, pp. 167.
- [23] PETERS, T. A. – FONTALVO, J. – VORSTMAN, M. A. G. – BENES, N. E. – VAN DAM, R. A. – VROON, Z. A. E. P. – VAN SOEST-VERCAMMEN E. L. J. – KEURENTJES, J. T. F., *J. of Membrane Science* **248** (2005) p. 73.
- [24] NIJMEIJER, A. – BLADERGROEN, B. J. – VERWEIJ, H., *Micro and Meso. Mater.* **25** (1998) p. 179.
- [25] LEE, D. – ZHANG, L. – OYAMA, S. T. – NIU, S. – SARAF, R. *F.J. of Membr. Sc.* **231** (2004) p. 117.
- [26] ROUESSAC, V. – FERREIRA, P. – DURAND, J., *Sep. and Pur. Technol.* **32** (2003) p. 37.
- [27] OYAMA, S. T. – LEE, D. – SUGIYAMA, S. – FUKUI, K. – IWASAWA, Y., *J. Mater. Sc.* **36** (2001) p. 5213.
- [28] LEE, D. – TED OYAMA, S., *J. of Membrane Science* **210** (2002) p. 291.